

Supporting Information

Porter et al. 10.1073/pnas.1718823114

SI Materials and Methods

Reagents. In general, chemicals used in buffers and crystallization were acquired from Fisher, Millipore Sigma, or Hampton Research and used without further purification. The inhibitor HPB was synthesized according to published procedures (1). Ricolinostat and ACY-1083 were the generous gift of Acetylon (now Celgene).

Protein Preparation. HDAC6 CD2 from *Danio rerio* (HDAC6) was recombinantly expressed using the MBP-tobacco etch virus (TEV)-z6CD2-pET28a(+) vector and purified as previously described with minor modifications (2). Briefly, HDAC6 was expressed by the *Escherichia coli* BL21 (DE3) strain (Stratagene) in 2× YT medium under the selection of 50 mg/L kanamycin. Expression was induced by 100 μM isopropyl β-L-1-thiogalactopyranoside (Gold Biotechnology), along with the addition of 200 μM ZnCl₂ at 16 °C. Cells were collected by centrifugation and stored at −80 °C before purification.

Pellets were thawed and resuspended in purification buffer [50 mM 4-(2-hydroxyethyl)-1-piperazine-ethanesulfonic acid (Hepes; pH 7.5), 300 mM KCl, 10% glycerol (vol/vol), 1 mM Tris (2-carboxyethyl)phosphine (TCEP)] and lysed by sonication. Lysate was clarified by centrifugation at 33,000 × g for 1 h at 4 °C. The supernatant was purified using an amylose column (New England BioLabs), and protein was eluted using 10 mM maltose. Protein was digested using recombinant His-TEV protease overnight at 4 °C while dialyzing in purification buffer + 20 mM imidazole. The digest was applied to an equilibrated nickel-nitrilotriacetic acid resin (Qiagen) to remove His-MBP and His-TEV, which were subsequently eluted with a 0–400 mM imidazole gradient in purification buffer. The HDAC6-containing fractions were concentrated to <10 mL over a 10,000 molecular weight cut-off filter unit (Millipore) and applied to a HiLoad Superdex 200-pg column in size exclusion buffer [50 mM Hepes (pH 7.5), 100 mM KCl, 5% glycerol (vol/vol), 1 mM TCEP]. Fractions containing pure HDAC6 were identified using SDS/PAGE, pooled, and concentrated to 14–20 mg/mL. Protein was flash-cooled in liquid nitrogen and stored at −80 °C before usage.

Crystallization. All HDAC6-inhibitor complexes were crystallized in sitting drops by the vapor diffusion method at 4 °C.

For cocrystallization of the HDAC6–HPB complex, a 350-nL drop of protein solution [10 mg/mL HDAC6, 50 mM Hepes (pH 7.5), 100 mM KCl, 5% glycerol (vol/vol), 1 mM TCEP, 5 mM HPB, 5% dimethyl sulfoxide (DMSO; vol/vol)] was added to a 350-nL drop of precipitant solution [200 mM ammonium chloride, 20% (wt/vol) PEG 3,350] and equilibrated against an 80-μL reservoir of precipitant solution. Hexagonal plate crystals appeared within 2 d.

For initial cocrystallization of the HDAC6–ACY-1083 complex, a 2-μL drop of protein solution [10 mg/mL HDAC6, 100 mM Hepes (pH 7.5), 100 mM KCl, 5% glycerol (vol/vol), 1 mM TCEP, 5 mM ACY-1083, 5% DMSO] was added to a 2-μL drop of precipitant solution [50 mM magnesium acetate,

100 mM sodium cacodylate (pH 6.5), 25% (wt/vol) PEG 8,000] and equilibrated against a 500-μL reservoir of precipitant solution. A few rhombus-shaped crystals appeared after 1 wk. These were crushed and used as a seed stock for a streak-seeding cocrystallization experiment using the same conditions, with the exception that a lower protein concentration was used (5 mg/mL HDAC6). This approach yielded many pyramid-shaped crystals within 1 d.

For cocrystallization of the HDAC6–Ricolinostat complex, a 350-μL drop of protein solution [10 mg/mL HDAC6, 50 mM Hepes (pH 7.5), 100 mM KCl, 5% glycerol (vol/vol), 1 mM TCEP, saturating Ricolinostat (*ca.* 1 mM), 5% DMSO (vol/vol)] was added to a 350-μL drop of precipitant solution [100 mM sodium citrate (pH 5.5), 16% (wt/vol) PEG 8,000] and equilibrated against an 80-μL reservoir of precipitant solution. Crystal plates appeared within 3 d.

For cocrystallization of HDAC6 with the *R*-stereoisomer of TSA, a 350-μL drop of protein solution [10 mg/mL HDAC6, 50 mM Hepes (pH 7.5), 100 mM KCl, 5% glycerol (vol/vol), 1 mM TCEP, 2 mM TSA, 5% DMSO] was added to 350 μL of precipitant solution [200 mM MgCl₂, 100 mM Bis(2-hydroxyethyl) amino-Tris(hydroxymethyl)methane (pH 6.5), 25% (wt/vol) PEG 3,350] and equilibrated against an 80-μL reservoir of precipitant solution. Thick crystal plates appeared within 2 d.

All crystals were soaked in a cryoprotectant solution containing mother liquor supplemented with 20% glycerol (HDAC6–TSA complex) or 15% (HDAC6–ACY-1083 complex), 20% (HDAC6–HPB complex), or 25% (HDAC6–Ricolinostat complex) ethylene glycol before flash-cooling in liquid nitrogen.

Data Collection and Structure Determination. X-ray diffraction data were collected from crystals on beamline 9-2 at the Stanford Synchrotron Radiation Laboratory, Stanford University (HDAC6–ACY-1083 and HDAC6–HPB complexes); beamline 4.2.2 at the Advanced Light Source, University of California, Berkeley (HDAC6–Ricolinostat complex); and beamline 24-ID-C at the Advanced Photon Source, Argonne National Laboratory (HDAC6–TSA complex). Data were indexed and integrated using either XDS (3) (HDAC6–TSA, HDAC6–ACY-1083, and HDAC6–Ricolinostat complexes) or iMosflm (4) (HDAC6–HPB complex) and scaled using Aimless in the CCP4 program suite (5). Data collection statistics are recorded in Table S1.

All crystal structures were solved by molecular replacement using the atomic coordinates of unliganded HDAC6 (PDB ID code 5EEM) (2) as a search model for rotation and translation function calculations using the program Phaser (6). Atomic models were constructed using the graphics program Coot (7), and crystallographic structure refinement was performed using Phenix (8). Inhibitor molecules were added in the later stages of refinement. Occasionally, maps displayed spurious electron density peaks that could not be satisfactorily modeled by ordered solvent, in which case these were left uninterpreted. The overall quality of each model was assessed using MolProbity (9) and PROCHECK (10). Final refinement statistics are recorded in Table S1.

- Lee JH, et al. (2015) Creation of a histone deacetylase 6 inhibitor and its biological effects [corrected]. *Proc Natl Acad Sci USA* 112:12005–12010, and correction (2015) 112:E5899.
- Hai Y, Christianson DW (2016) Histone deacetylase 6 structure and molecular basis of catalysis and inhibition. *Nat Chem Biol* 12:741–747.
- Kabsch W (2010) XDS. *Acta Crystallogr D Biol Crystallogr* 66:125–132.

- Battye TGG, Kontogiannis L, Johnson O, Powell HR, Leslie AGW (2011) iMOSFLM: A new graphical interface for diffraction-image processing with MOSFLM. *Acta Crystallogr D Biol Crystallogr* 67:271–281.
- Winn MD, et al. (2011) Overview of the CCP4 suite and current developments. *Acta Crystallogr D Biol Crystallogr* 67:235–242.
- McCoy AJ, et al. (2007) Phaser crystallographic software. *J Appl Cryst* 40:658–674.

7. Emsley P, Lohkamp B, Scott WG, Cowtan K (2010) Features and development of Coot. *Acta Crystallogr D Biol Crystallogr* 66:486–501.
8. Adams PD, et al. (2010) PHENIX: A comprehensive Python-based system for macromolecular structure solution. *Acta Crystallogr D Biol Crystallogr* 66:213–221.

9. Chen VB, et al. (2010) MolProbity: All-atom structure validation for macromolecular crystallography. *Acta Crystallogr D Biol Crystallogr* 66:12–21.
10. Laskowski RA, MacArthur MW, Moss DS, Thornton JM (1993) PROCHECK: A program to check the stereochemical quality of protein structures. *J Appl Cryst* 26:283–291.

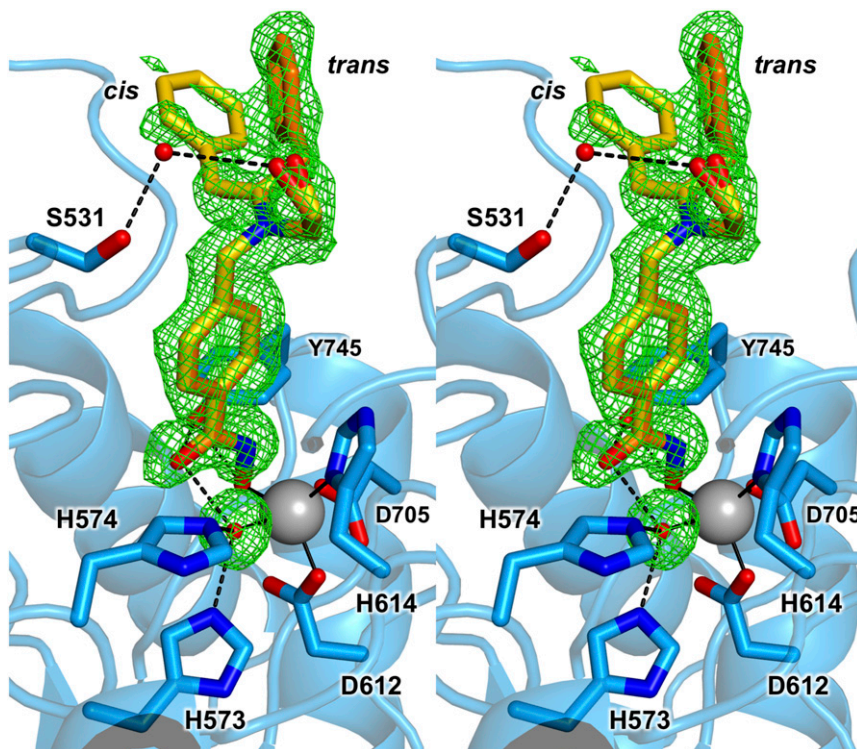


Fig. S1. Stereoview of Fig. 1A showing a simulated annealing omit map (green, contoured at 2.0σ) for *cis* (yellow) and *trans* (orange) conformations of HPB bound to HDAC6. Omit density is also shown for the water molecule (red sphere) bound to the Zn²⁺ ion (gray sphere). Metal coordination and hydrogen bond interactions are indicated by solid and dashed black lines, respectively.

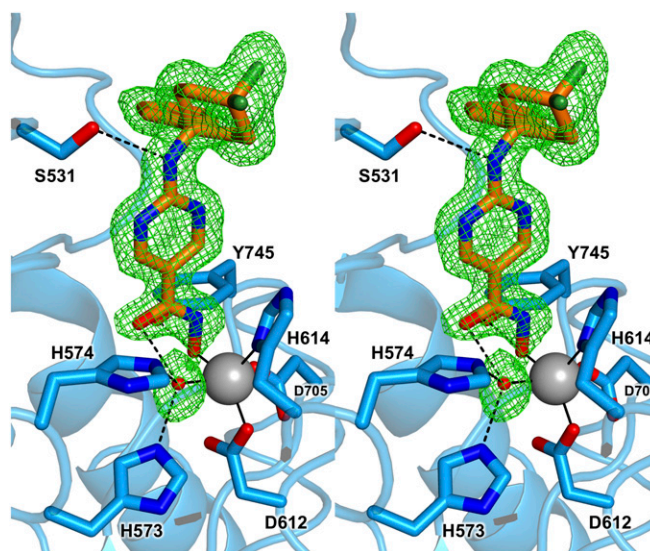


Fig. S2. Stereoview of Fig. 2A showing a simulated annealing omit map (green, contoured at 2.5σ) for ACY-1083 (orange) and the water molecule (red sphere) bound to the Zn²⁺ ion (large gray sphere) in the active site of HDAC6. Metal coordination and hydrogen bond interactions are indicated by solid and dashed black lines, respectively.

Table S1. Data collection and refinement statistics for HDAC6-inhibitor complexes

Inhibitor	TSA	HPB	Ricolinostat	ACY-1083
Unit cell				
Space group	$P2_1$	$P22_12_1$	$P2_12_12_1$	$C22_1$
a, b, c, Å	48.4, 69.6, 50.2	51.7, 84.0, 94.6	87.2, 88.0, 119.0	97.8, 173.4, 149.1
$\alpha, \beta, \gamma, ^\circ$	90.0, 110.42, 90.0	90.0, 90.0, 90.0	90.0, 90.0, 90.0	90.0, 90.0, 90.0
Data collection				
Wavelength, Å	0.97920	0.97946	1.00003	0.97946
Resolution, Å	47.04–1.05	62.79–1.82	49.3–1.70	48.91–1.75
Total/unique no. of reflections	455,704/138,710	207,193/37,115	696,967/101,104	864,102/127,773
$R_{\text{merge}}^{*,\dagger}$	0.067 (0.689)	0.103 (0.343)	0.139 (0.789)	0.189 (0.930)
$R_{\text{p.i.m.}}^{*,\ddagger}$	0.043 (0.460)	0.047 (0.155)	0.057 (0.333)	0.078 (0.391)
$CC_{1/2}^{*,\S}$	0.998 (0.591)	0.995 (0.90)	0.996 (0.842)	0.989 (0.746)
$I/\sigma(I)^*$	11.1 (1.9)	11.7 (4.7)	14.1 (2.7)	8.0 (2.2)
Redundancy*	3.3 (3.1)	5.6 (5.7)	6.9 (6.5)	6.8 (6.6)
Completeness*, %	95.6 (89.8)	99.1 (99.3)	99.9 (100.)	100.0 (99.9)
Refinement				
No. of reflections used in refinement/test set	138,678/6,928	37,057/1,812	100,931/5,089	127,726/6,481
$R_{\text{work}}^{*,\P}$	0.113 (0.226)	0.149 (0.179)	0.184 (0.206)	0.163 (0.255)
$R_{\text{free}}^{*,\P}$	0.132 (0.237)	0.173 (0.233)	0.209 (0.240)	0.189 (0.275)
No. of nonhydrogen atoms				
Protein	2,960	2,839	5,682	8,581
Ligand	109	127	186	247
Solvent	368	416	552	794
Average B-factors, Å ²				
Protein	9	11	14	16
Ligand	22	28	21	26
Solvent	25	23	23	25
rmsd from ideal geometry				
Bonds, Å	0.009	0.012	0.019	0.011
Angles, °	1.16	0.89	1.24	1.11
Ramachandran plot, [#] %				
Favored	97.45	97.16	96.47	97.29
Allowed	2.55	2.84	3.53	2.53
Disallowed	0.00	0.00	0.00	0.19
PDB ID code	5WGI	5WGK	5WGL	5WGM

*Values in parentheses refer to the data from the highest resolution shell.

[†] $R_{\text{merge}} = \sum_{hkl} \sum_i |I_{i,hkl} - \langle I \rangle_{hkl}| / \sum_{hkl} \sum_i I_{i,hkl}$, where $\langle I \rangle_{hkl}$ is the average intensity calculated for reflection hkl from replicate measurements.

[‡] $R_{\text{p.i.m.}} = \text{precision-indicating merging R factor} = (\sum_{hkl} (1/(N-1))^{1/2} \sum_i |I_{i,hkl} - \langle I \rangle_{hkl}|) / \sum_{hkl} \sum_i I_{i,hkl}$, where $\langle I \rangle_{hkl}$ is the average intensity calculated for reflection hkl from replicate measurements and N is the number of reflections.

[§]Pearson correlation coefficient between random half-datasets.

[¶] $R_{\text{work}} = \sum ||F_o| - |F_c|| / \sum |F_o|$ for reflections contained in the working set. $|F_o|$ and $|F_c|$ are the observed and calculated structure factor amplitudes, respectively. R_{free} is calculated using the same expression for reflections contained in the test set held aside during refinement.

[#]Calculated with PROCHECK (1).

1. Laskowski RA, MacArthur MW, Moss DS, Thornton JM (1993) PROCHECK: A program to check the stereochemical quality of protein structures. *J Appl Cryst* 26:283–291.